

Electronic Supplementary Material (ESI) for Chem. Comm.

Ultra-long Nanoribbons Formation by Self-assembly of Carbon Dots and Anionic Oligomers for Multi-colored Fluorescence and Electrical Conduction†

Guiyang Zhang,^{‡,a} Manqing Yan,^{‡,a} Xiyao Teng,^a Hong Bi^{*a} Yuyan Han,^c Mingliang Tian,^c Mingtai Wang^{*b}

Supporting Information

Table of Contents

I. Experimental Details

- Chemicals and Materials
- Preparation and Purification of C-dots
- Synthesis of (PS-PSS)/C-dots Nanoribbons
- Characterizations
- Quantum Yields (QYs) Measurement

II. Supplemental Figures of C-dots

Figure S1. (a) TEM image of the C-dots, the inset is a HRTEM image of an individual C-dots. (b) Size distribution histogram of C-dots according to TEM.

III. Supplemental Figures of (PS-PSS)/C-dots Nanoribbons

Figure S2. TEM images of the control product without adding C-dots, the obtained PS-PSS microspheres at (a) 2 h and (b) 4 h, respectively.

Figure S3. (a) TEM image of the (PS-PSS)/C-dots nanoribbons obtained at 2 h. (b) HRTEM images of an individual nanoribbon created within 5 seconds. (c) AFM image of an individual (PS-PSS)/C-dots nanoribbon. (d) The height profile along the line arrowed in (c).

Figure S4. HRTEM images of (a) an individual nanoribbon under the high-energy electron beam irradiation of 200 kV from the electron microscope created within 10 seconds. (b) A partially destroyed nanoribbon after the high-energy electron beam irradiation of 200 kV.

Figure S5. (i,ii,iii,iv) Fluorescence microscopy images of the (PS-PSS)/C-dots nanoribbons in bright field, blue, green, and red channels. (a,b,c,d) Fluorescence microscopy images of the aggregated C-dots released from the (PS-PSS)/C-dots nanoribbons when dissolved in THF.

Figure S6. ¹H NMR spectrum of the supernatant after (PS-PSS)/C-dots nanoribbons dissolved in CDCl₃.

Figure S7. The digital photographs of the dispersion of (PS-PSS)/C-dots nanoribbons in ethanol stored at room temperature for 1 day, 3 days, and 7 days, respectively.

Figure S8. THF GPC traces recorded for (a) (PS-PSS)/C-dots nanoribbons ($M_n = 1700$ g/mol, $M_w/M_n = 1.23$) and (b) PS-PSS microspheres ($M_n = 2500$ g/mol, $M_w/M_n = 1.06$).

Figure S9. MALDI-TOF mass spectrum (negative mode) of remanent of the (PS-PSS)/C-dots nanoribbons after dissolved in H₂O. The observed mass of peaks, for example, the major peak at

2219.7 Da is assigned to 17 St repeating units and 2 NaSS units plus one end group (–OH) and Na⁺ from the cationizing agent NaTFA.

Figure S10. (a,b) TEM images of the (PS-PSS)/C-dots nanoribbons obtained at 3 h, the inset in (b) is the corresponding SAED pattern of an individual nanoribbon. (c,d) TEM images of the reaction product obtained at 4 h, the inset in (d) is the corresponding SAED pattern of the part showing the stacking fault.

Figure S11. (Upper) Schematic preparation procedures of (PS-PSS)/C-dots nanoribbons and PS-PSS microspheres, respectively. (Lower) Schematic representation of the building blocks and their self-assembly orientation in an individual (PS-PSS)/C-dots nanoribbon.

Figure S12. The micrographs of an individual nanoribbon with (a) the width of 1.197 μm and (b) the length of 118.6 μm ; (c) between two electrodes and (d) in an OFET device.

Figure S13. (A) SEM and (B) TEM images of the Ag-(PS-PSS)/C-dots nanobelts.

I. Experimental Details

Chemicals and Materials. Styrene (St) from Aldrich was passed through a basic alumina column, then vacuum distilled from calcium hydride (CaH₂) and stored at -20 °C prior to use. 4-styrenesulfonic acid sodium salt (NaSS) and potassium persulphate (KPS) from Sinopharm were used as received.

Preparation and Purification of C-Dots. Here we present a general approach for the preparation of high quality C-dots through pyrolysis of konjac flour (KF) as previously reported by our lab,^[S1] only with a simple extraction by ethanol and dichloromethane. In a typical process, firstly, 1 g KF was pyrolyzed under air atmosphere at 470 °C for 1.5 h with a heating rate of 5 °C min⁻¹. Secondly, the black, carbonized solid was ground into fine powder and then mixed with 20 mL of ethanol under stirring over night to extract the C-dots from it. The as-prepared C-dots possessed a positive Zeta potential of ca. + 3.8 mV in a mixture of ethanol/water (4/1, v/v).

Synthesis of (PS-PSS)/C-dots Nanoribbons. In a typical synthesis, 50 mg of potassium persulphate (KPS) and 6 mg of 4-styrenesulfonic acid sodium salt (NaSS) were dissolved in a mixture of ethanol/water (16.5 ml/4.5 ml) in a 25-mL three-neck flask equipped with a reflux condenser and a Teflon-coated magnetic stirring bar. This system was heated to 70 °C and kept for 2 min under magnetic stirring. Subsequently, 0.2 mL of a styrene was added into the flask, and 2 min later, 3.0 mL of the C-Dots solution in ethanol (0.15 mg/mL) was added dropwise. Then the reaction temperature was kept at 70 °C for 2 h before the product was collected. The product was obtained by precipitation in cold diethyl ether twice, centrifugation, and then washing with a mixture of ethanol/water (4/1, v/v)

three times as well as ethanol one time. As a control, a sample comprising PS- PSS copolymers was prepared by a similar procedure except adding C-dots to the reaction mixture.

Characterizations. The morphology of the products was observed on a transmission electron microscope (TEM, JEM-2100). The sample for TEM observations was prepared by dropping 10 μ L of the suspension in ethanol on copper grids. The Fourier Transform Infrared (FT-IR), Raman and ultraviolet visible (UV-Vis) spectra of samples were recorded using NEXUS-870 spectrometer, LabRAM HR800 Raman laser Raman spectroscopy and UV759 spectrophotometer, respectively. PL emission measurements were performed using a fluorescence spectrophotometer (F-4500, Hitachi). Fluorescence microscopy images of the (PS-PSS)/C-dots nanoribbons were taken by Olympus IX-51 (FM). Molecular weights and polydispersity were determined by gel permeation chromatography (GPC) equipped with a Waters 1515 pump and a Waters 2414 differential refractive index detector (set at 30 °C). It used a series of two linear Styragel columns (HR2 AND HR4) at an oven temperature of 45°C. The eluent was THF at a flow rate of 1.0 ml/min. A series of low polydispersity polystyrene standards were employed for calibration. Matrix assisted laser desorption ionization time of flight mass spectrometry (MALDI TOF MS) was performed on an Applied Biosystems Voyager DE-STR MALDI-TOF equipped with a nitrogen laser (337 nm). The mass spectra of negative ions were collected in the linear mode under an acceleration voltage of 25 kV and a delay time of 350 ns. Trans-2-[3-(4-tert-butyl-phenyl)-2-methyl-2-propenylidene] malononitrile (DCTB) was used as MALDI matrix and sodium trifluoroacetate (NaTFA) was used as a cationizing agent.

The OFET device was fabricated using FEI NanoLab 600i SEM/FIB dual beams system. Two platinum (Pt) stripes (width: 240 nm; thickness: 150 nm) acting as the source and drain electrodes were deposited on a randomly selected nanoribbon on a heavily doped Si substrate with a 300 nm SiO₂ layer, where a small beam current of 2.3 nA was applied under 30 kV acceleration voltage in order to avoid the milling of the nanoribbon.

Quantum Yield (QYs) Measurement

Rhodamine B in ethanol (QY = 0.65, from literature^[S2]) was selected as a control standard. The QYs of C-dots and nanoribbons were estimated according to the follow equation 1:

$$\Phi = \Phi_r \times \frac{I}{A} \times \frac{A_r}{I_r} \times \frac{n^2}{n_r^2} \quad (1)$$

Where the Φ is the QY, I is the integrated PL emission intensity (excited at 335 nm for C-dots and at 268 nm for nanoribbons, respectively), n is the refractive index (= 1.3614 for ethanol), and A is the absorbance value at the excitation wavelength of 335 nm and 268 nm in ethanol, respectively (the value of A should be less than 0.1 at the excitation wavelength). The subscript “r” refers to the standards.

Table S1. QYs of the C-dots and nanoribbons dispersed in ethanol, respectively

Samples	Integrated emission intensity (I)	Abs. 335 nm (A)	Refractive index of solvent (n)	QY (Φ)
Rhodamine B	55280	0.0087	1.362	0.65
C-dots	141417	0.07975	1.362	0.18
Samples	Integrated emission intensity (I)	Abs. 268 nm (A)	Refractive index of solvent (n)	QY (Φ)
Rhodamine B	20153	0.0389	1.362	0.65
Nanoribbons	10075	0.0742	1.362	0.17

II. Supplemental Figures of C-dots

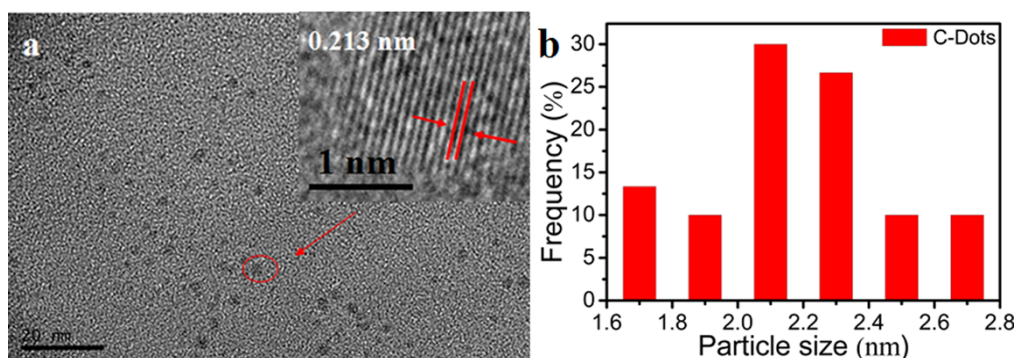


Figure S1. (a) TEM image of the C-dots, the inset is a HRTEM image of an individual C-dots. (b) Size distribution histogram of C-dots according to TEM.

III. Supplemental Figures of (PS-PSS)/C-dots Nanoribbons

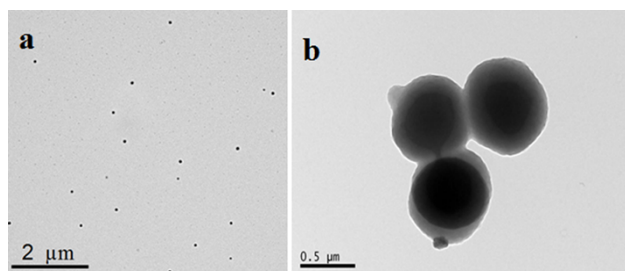


Figure S2. TEM images of the control product without adding C-dots, the obtained PS-PSS microspheres at (a) 2 h and (b) 4 h, respectively.

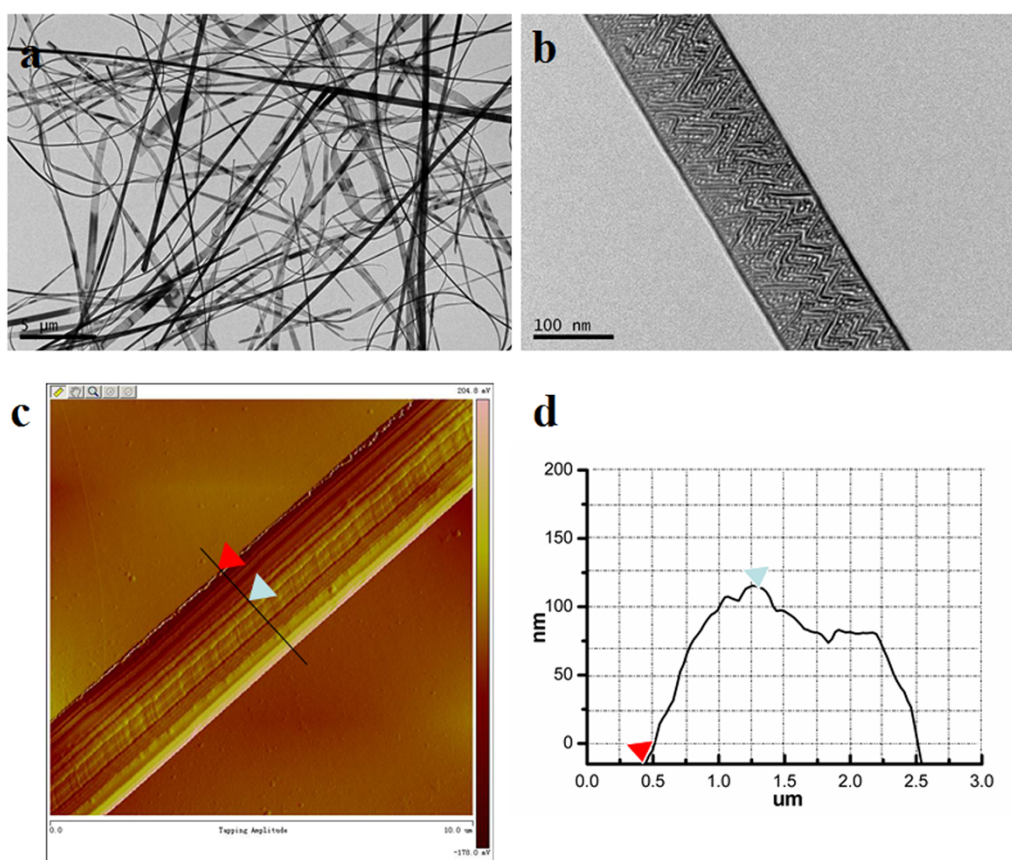


Figure S3. (a) TEM image of the (PS-PSS)/C-dots nanoribbons obtained at 2 h. (b) HRTEM images of an individual nanoribbon created within 5 seconds. (c) AFM image of an individual (PS-PSS)/C-dots nanoribbon. (d) The height profile along the line arrowed in (c).

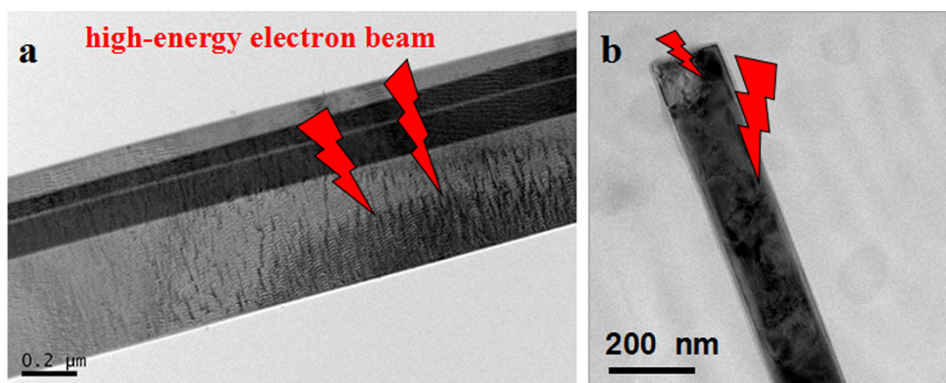


Figure S4. HRTEM images of (a) an individual nanoribbon under the high-energy electron beam irradiation of 200 kV from the electron microscope created within 10 seconds. (b) A partially destroyed nanoribbon after the high-energy electron beam irradiation of 200 kV.

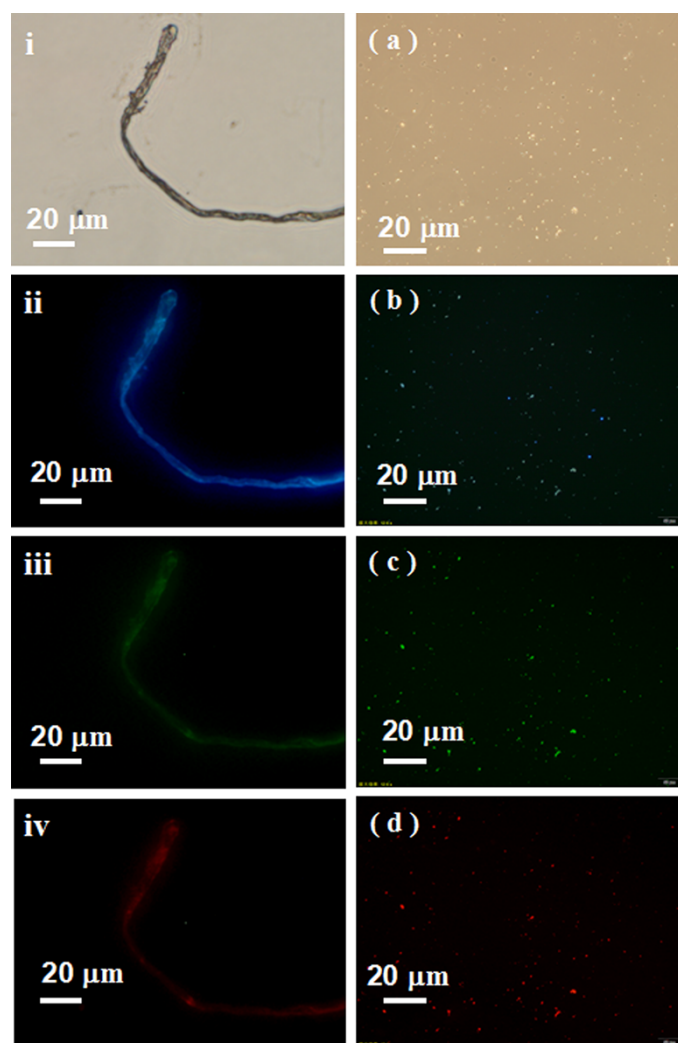


Figure S5. (i,ii,iii,iv) Fluorescence microscopy images of the (PS-PSS)/C-dots nanoribbons in bright field, blue, green, and red channels. (a,b,c,d) Fluorescence microscopy images of the aggregated C-dots released from the (PS-PSS)/C-dots nanoribbons when dissolved in THF.

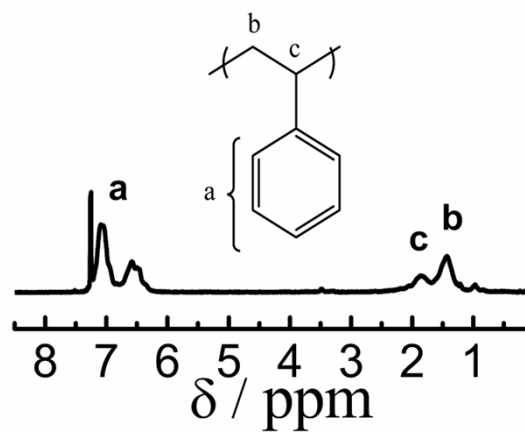


Figure S6. ^1H NMR spectrum of the supernatant after (PS-PSS)/C-dots nanoribbons dissolved in CDCl_3 .

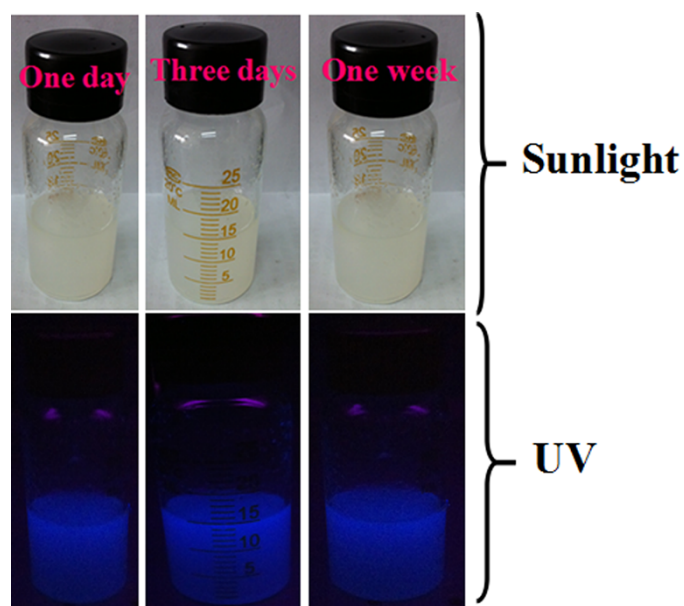


Figure S7. The digital photographs of the dispersion of (PS-PSS)/C-dots nanoribbons in ethanol stored at room temperature for 1 day, 3 days, and 7 days, respectively.

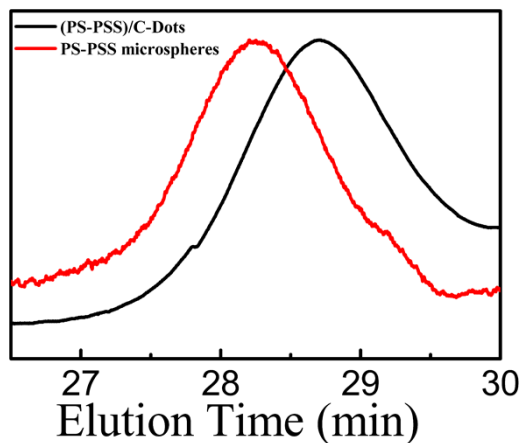


Figure S8. THF GPC traces recorded for (a) (PS-PSS)/C-dots nanoribbons ($M_n = 1700$ g/mol, $M_w/M_n = 1.23$) and (b) PS-PSS microspheres ($M_n = 2500$ g/mol, $M_w/M_n = 1.06$).

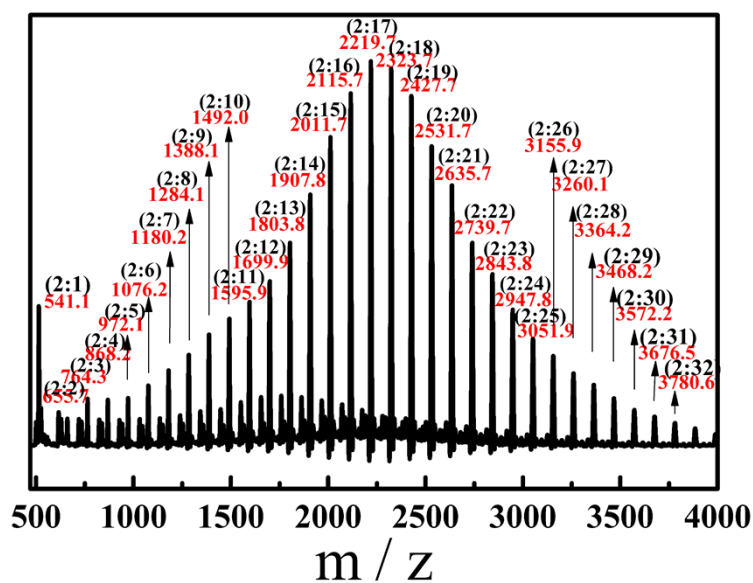


Figure S9. MALDI-TOF mass spectrum (negative mode) of remanent of the (PS-PSS)/C-dots nanoribbons after dissolved in H_2O . The observed mass of peaks, for example, the major peak at 2219.7 Da is assigned to 17 St repeating units and 2 NaSS units plus one end group ($-OH$) and Na^+ from the cationizing agent NaTFA.

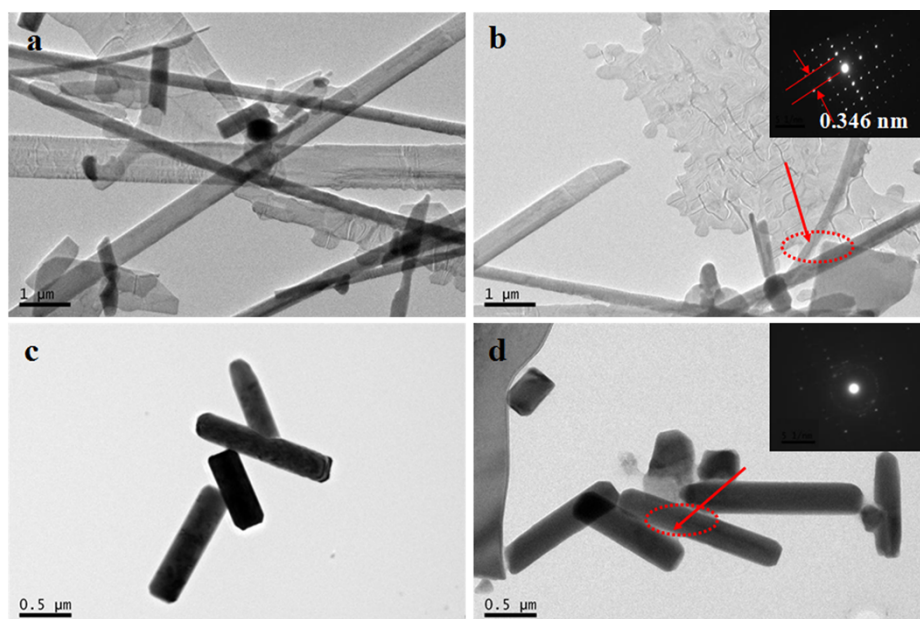


Figure S10. (a,b) TEM images of the (PS-PSS)/C-dots nanoribbons obtained at 3 h, the inset in (b) is the corresponding SAED pattern of an individual nanoribbon. (c,d) TEM images of the reaction product obtained at 4 h, the inset in (d) is the corresponding SAED pattern of the part showing the stacking fault.

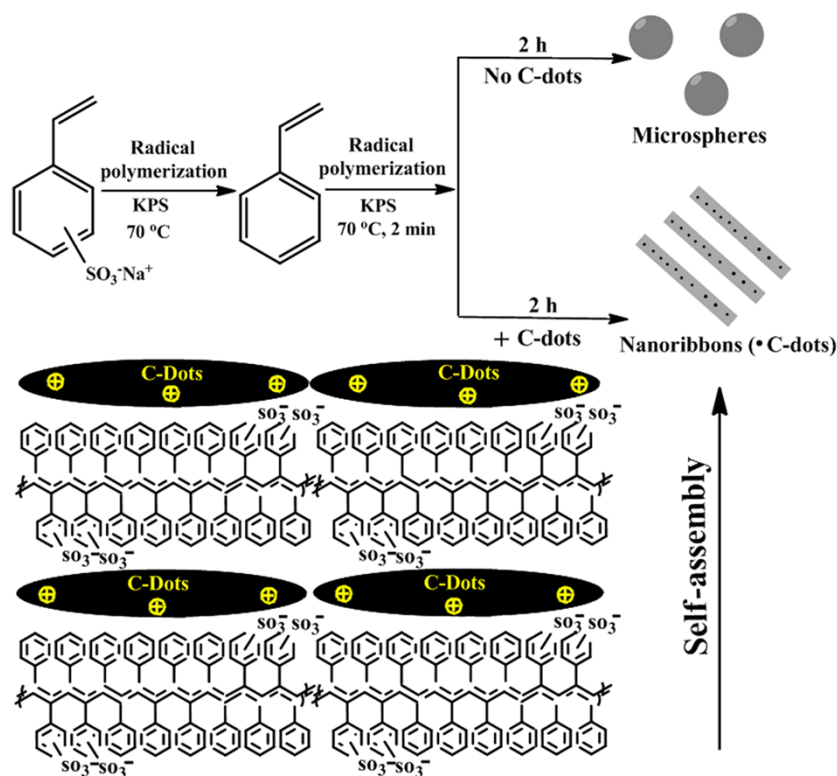


Figure S11. (Upper) Schematic preparation procedures of (PS-PSS)/C-dots nanoribbons and PS-PSS microspheres, respectively. (Lower) Schematic representation of the building blocks and their self-assembly orientation in an individual (PS-PSS)/C-dots nanoribbon.

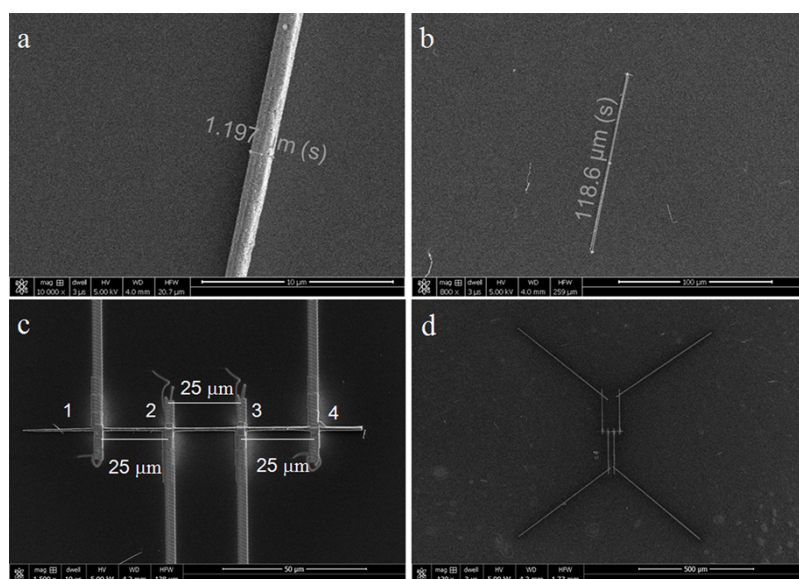


Figure S12. The micrographs of an individual nanoribbon with (a) the width of $1.197 \mu\text{m}$ and (b) the length of $118.6 \mu\text{m}$; (c) between two electrodes and (d) in an OFET device.

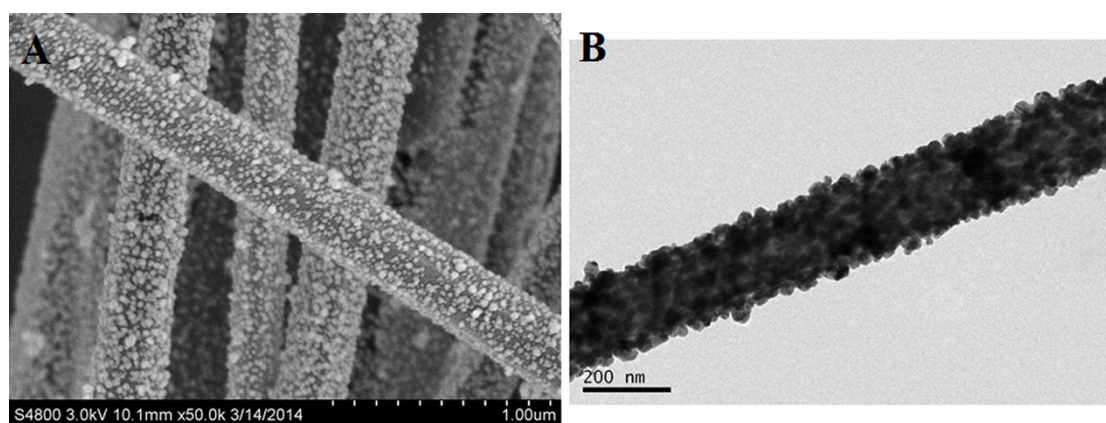


Figure S13. (A) SEM and (B) TEM images of the Ag-(PS-PSS)/C-dots nanobelts.

Notes and references

[S1] X. Teng, C. Ma, C. Ge, M. Yan, J. Yang, Y. Zhang, P. C. Morais and H. Bi, *J. Mater. Chem. B*, 2014, **2**, 4631.

[S2] R. F. Kubin and A. N. Fletcher, *J. Lumin.* 1982, **27**, 455.